Detection of Increased ^{64}Cu Uptake by Human Copper Transporter 1 Gene Overexpression Using PET with $^{64}CuCl_2$ in Human Breast Cancer Xenograft Model

Kwang Il Kim[1], Su Jin Jang[1], Ju Hui Park[1], Yong Jin Lee[1], Tae Sup Lee[1], Kwang Sun Woo[1], Hyun Park[1], Jae Gol Choe[2], Gwang Il An[1], and Joo Hyun Kang[1]

[1]*Molecular Imaging Research Center, Korea Institute of Radiological and Medical Sciences, Seoul, Korea; and* [2]*Department of Nuclear Medicine, Korea University Anam Hospital, Korea University College of Medicine, Seoul, Korea*

Copper is an essential cofactor for a variety of biochemical processes including oxidative phosphorylation, cellular antioxidant activity, and elimination of free radicals. The copper transporter 1 is known to be involved in cellular uptake of copper ions. In this study, we evaluated the utility of human copper transporter 1 (*hCTR1*) gene as a new reporter gene for ^{64}Cu PET imaging. **Methods:** Human breast cancer cells (MDA-MB-231) were infected with a lentiviral vector constitutively expressing the *hCTR1* gene under super cytomegalovirus promoter, and positive clones (MDA-MB-231-hCTR1) were selected. The expression of *hCTR1* gene in MDA-MB-231-hCTR1 cells was measured by reverse transcription polymerase chain reaction, Western blot, and ^{64}Cu uptake assay. To evaluate the cytotoxic effects induced by hCTR1 expression, the dose-dependent cell survival rate after treatment with cisplatin (*Cis*-diaminedichloroplatinum (II) [CDDP]) was determined by 3-(4,5-dimethylthiazol-2-yl)-2,5-diphenyltetrazolium bromide (MTT) assay and trypan blue dye exclusion. Small-animal PET images were acquired in tumor-bearing mice from 2 to 48 h after an intravenous injection of ^{64}Cu. **Results:** The *hCTR1* gene expression in MDA-MB-231-hCTR1 cells was confirmed at the RNA and protein expression and the cellular ^{64}Cu uptake level. MTT assay and trypan blue dye exclusion showed that the cell viability of MDA-MB-231-hCTR1 cells decreased more rapidly than that of MDA-MB-231 cells after treatment with CDDP for 96 or 72 h, respectively. Small-animal PET imaging revealed a higher accumulation of ^{64}Cu in MDA-MB-231-hCTR1 tumors than in MDA-MB-231 tumors. With respect to the biodistribution data, the percentage injected dose per gram of ^{64}Cu in the MDA-MB-231 tumors and MDA-MB-231-hCTR1 tumors at 48 h after ^{64}Cu injection was 2.581 ± 0.254 and 5.373 ± 1.098, respectively. **Conclusion:** An increase in ^{64}Cu uptake induced by the expression of *hCTR1* gene was demonstrated in vivo and in vitro, suggesting the potential use of *hCTR1* gene as a new imaging reporter gene for PET with $^{64}CuCl_2$.

Key Words: hCTR1; reporter gene; ^{64}Cu; PET; cisplatin

J Nucl Med 2014; 55:1692–1698
DOI: 10.2967/jnumed.114.141127

Copper plays an essential role in many biologic processes such as mitochondrial oxidative phosphorylation, detoxification of free radicals, neurotransmitter synthesis, cross-linking of connective tissue, and iron metabolism (*1*). Menkes and Wilson diseases result from disruption of the copper homeostatic mechanisms due to a genetic disorder. Menkes disease is a copper-deficiency disorder affecting the brain (*2*), and Wilson disease is a genetic disorder of excess copper accumulation in the liver due to loss of ATP7B, a copper-transporting ATPase (*3*). Therefore, the level of copper in cells and tissue must be tightly regulated. The gene (copper transporter 1 [*CTR1*]) encoding a high-affinity copper transport protein was first identified and characterized in yeast (*4*). Human and mouse CTR1 homologs were identified by a database homology search and a complementation study of yeast mutants (*5,6*). Lee et al. reported that human *CTR1* (*hCTR1*) gene was exogenously expressed in an embryonic kidney cell line (HEK293), and it played a role in copper uptake across the cell membrane in a time- and concentration-dependent manner (*7*).

Advances in molecular imaging techniques could significantly contribute to new drug development by reducing the research and development costs and to the field of basic life sciences (*8*). For the development of nuclear medicine imaging including scintigraphy, SPECT, and PET, the production of new radioisotopes with proper chemical and physical characteristics is essential. Of the various radioisotopes, ^{64}Cu is the most widely studied copper radionuclide, and it can be produced via the ^{64}Ni (p,n) ^{64}Cu reaction using a cyclotron in a carrier-free state. ^{64}Cu with a half-life of 12.7 h is a useful radiometal for PET imaging and for therapeutic applications with decay modes of β^+ (19%), electron capture (41%), and β^- (40%) (*9*).

Molecular-genetic imaging is based on the expression of imaging reporter genes, which are developed for optical, MR, and nuclear medicine modalities. Nuclear medicine reporter gene paradigms fall into 3 categories—that is, enzyme based (herpes simplex virus type 1 thymidine kinase gene), receptor based (dopamine receptor gene), and transporter based (sodium iodide symporter gene [*NIS*]) (*8*). Because of the wide availability of its substrates—that

Received Apr. 3, 2014; revision accepted Jul. 11, 2014.
For correspondence or reprints contact either of the following:
Joo Hyun Kang, Molecular Imaging Research Center, Korea Institute of Radiological and Medical Sciences, 75, Nowon-ro, Nowon-gu, Seoul 139-706, Korea.
E-mail: kang2325@kirams.re.kr
Gwang Il An, PhD, Molecular Imaging Research Center, Korea Institute of Radiological and Medical Sciences, 75, Nowon-ro, Nowon-gu, Seoul 139-706, Korea.
E-mail: gwangil@kirams.re.kr
Published online Aug. 4, 2014.

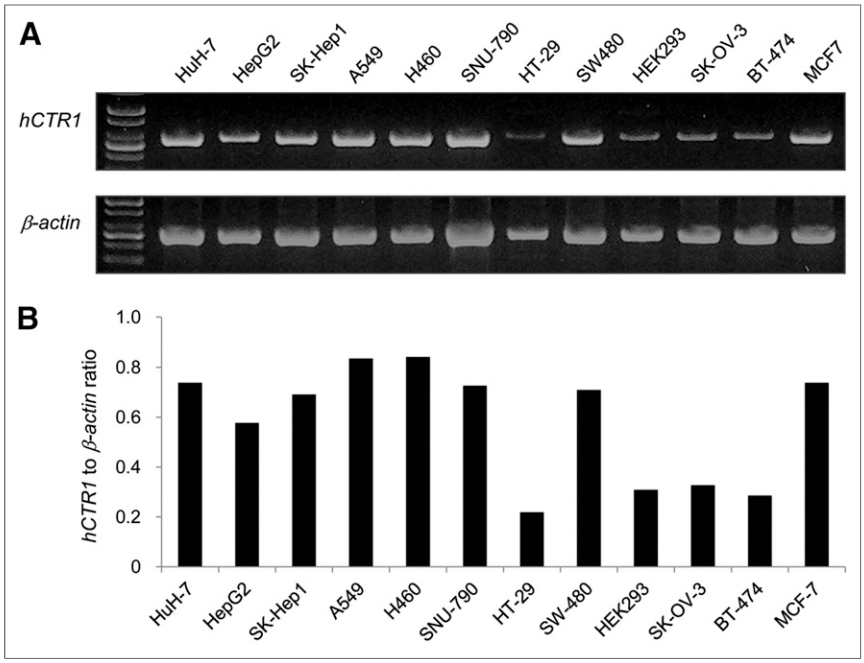

FIGURE 1. Expression of endogenous *hCTR1* gene in cells derived from various organs. (A) Endogenous *hCTR1* expression was analyzed by PCR using specific primers. *hCTR1*-specific PCR product was detected. (B) Semiquantitative analysis of endogenous *hCTR1* expression was performed with *β-actin* as internal control.

is, radioiodines, ^{99m}Tc-pertechnetate, and ^{188}Re-perrhenate—*NIS* can be used as a therapeutic gene with ^{188}Re-perrhenate or ^{131}I and as an imaging reporter gene with ^{99m}Tc-pertechnetate or ^{124}I (*10–12*). The *hCTR1* gene could be used as a therapeutic gene and as a nuclear medicine reporter gene of the transporter type similar to NIS because of the physical characteristics of the ^{64}Cu radioisotope (*9*). Therefore, NIS and hCTR1 have something in common with use of the radioisotope itself without complex synthesis as a substrate and application to therapeutic genes according to the physical characteristics of radioisotope (*8*).

It has been reported that CTR1 mediates the initial cellular influx of platinum-containing drugs—including cisplatin, carboplatin, oxaliplatin, and transplatin—and plays an important role for responsiveness to cisplatin in vivo as well as in vitro (*13*). The cellular uptake of cisplatin was enhanced by the overexpression of *hCTR1* gene (*14*), and hCTR1 expression level may be applicable for the prediction of tumor cell sensitivity to the platinum-containing drugs.

In this study, we cloned the *hCTR1* gene and constructed the hCTR1-expressing cell line (MDA-MB-231-hCTR1) to evaluate the utility of *hCTR1* gene as a new PET imaging reporter gene. In vitro–enhanced cytotoxic effects of cisplatin, a higher accumulation of ^{64}Cu in xenografted tumors on PET images, and a biodistribution study indicated the expression of exogenous *hCTR1* gene.

MATERIALS AND METHODS

Cell Lines

Human hepatoma cell lines (HuH-7, HepG2, SK-Hep1), human lung cancer cell lines (A549, H460), human colon cancer cell lines (HT-29, SW-480), human embryonic kidney cell line (HEK-293), human ovarian cancer cell line (SK-OV-3), human breast cancer cell lines (BT-474, MCF-7, MDA-MB-231), and human glioblastoma cell line (U87MG) were purchased from the American Type Culture Collection. A human thyroid cancer cell line (SNU-790) was purchased from the Korean Cell Line Bank. HuH-7, HepG2, SK-Hep1, HT-29, SW-480, HEK-293, SK-OV-3, and U87MG cells were grown in Dulbecco modified Eagle medium (WelGENE), supplemented with 10% heat-inactivated fetal bovine serum (FBS, Invitrogen) and antibiotics (penicillin [100 units/mL] and streptomycin [100 μg/mL]) (Invitrogen) at 37°C in a 5% CO2 humidified atmosphere. Also, A549, H460, BT-474, MCF-7, and MDA-MB-231 cells were cultured in RPMI 1640 medium (WelGENE) supplemented with 10% FBS (Invitrogen) and antibiotics (Invitrogen).

Establishment of Stable hCTR1-Expressing Cell Lines Using Lentiviral Vector

The hCTR1 lentivirus was custom-made by GenTarget, Inc. Briefly, the hCTR1 (GenBank sequence no. U83460.1) coding sequence was subcloned into GenTarget's lentiviral expression vector. The subcloned insert was constitutively expressed under a super cytomegalovirus promoter. The vector contains a green fluorescent protein–blasticidin deaminase fusion gene under the control of a Rous sarcoma virus promoter as a dual marker. The sequence-verified lentiviral expression vector was cotransfected with lentiviral packaging plasmids into a lentivirus production cell line.

One day before infection with lentiviral vector, cells were seeded on 6-well plates at a density of 5×10^5 cells/well. After overnight culture, the cells were preincubated with serum-free medium for 4 h. The cells were infected by exposing the cell monolayer to the lentivirus for 6 h in the presence of Polybrene (8 μg/mL; Sigma) with gentle shaking every 30 min. After 6 h of incubation, lentivirus-infected cells were added to the complete medium and grown overnight. After 48 h of incubation in the complete medium, positive clones (MDA-MB-231-hCTR1, U87MG-hCTR1) were selected using blasticidin S antibiotic (100 μg/mL).

In Vitro ^{64}Cu Uptake Assay

Radioactive copper (^{64}Cu) was produced from a 50-MeV cyclotron (Scantronics Co.) at the Korea Institute of Radiologic and Medical Sciences using enriched nickel (^{64}Ni, Isoflex Co., 99%) as the target material (*15*). The average specific activity of ^{64}Cu was 1,110 MBq (30 mCi) of copper per microgram in the form of $CuCl_2$ in 0.1 M HCl. Uptake of ^{64}Cu into cells was determined under modified conditions as described by Lee et al. (*7*). In brief, ^{64}Cu uptake level was measured by incubating the cells with 74 kBq (2 μCi) of ^{64}Cu in 2 mL of serum-free medium at 37°C for 5–120 min. After incubation, the cells were quickly washed twice (<15 s) with 2 mL of ice-cold phosphate-buffered saline. The cells were detached with 500 μL of trypsin, and the radioactivity was measured by γ counter (1480 WIZARD; PerkinElmer). ^{64}Cu uptake was expressed as the percentage injected dose (%ID).

Reverse Transcription Polymerase Chain Reaction (RT-PCR) and Western Blot Analysis

The total RNA was prepared from the cells using the Easy-spin (DNA free) Total RNA Extraction Kit (iNtRON Biotechnology). First

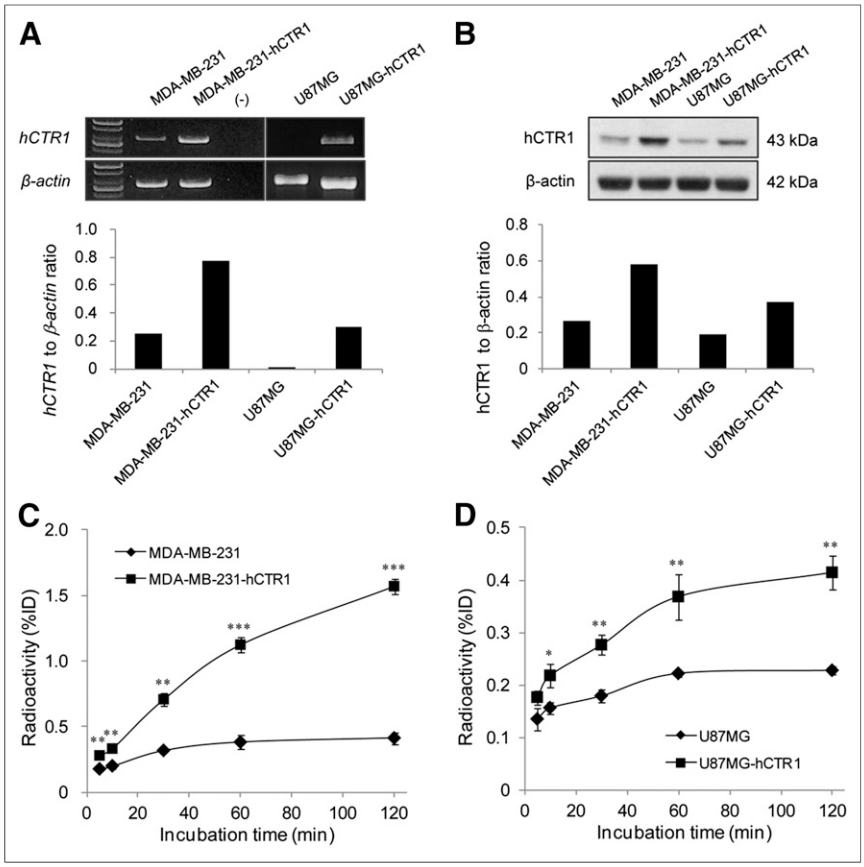

FIGURE 2. Confirmation of exogenous hCTR1 expression. (A) RT-PCR analysis of *hCTR1* gene expression. (-) indicates PCR products without template DNA. (B) Western blot analysis of hCTR1 expression using anti-CTR1 antibodies. Semiquantitative analysis of expression of exogenously transduced hCTR1 was normalized to β-actin as internal control in both RT-PCR and Western blot. (C and D) In vitro ^{64}Cu uptake assay. Measurement of hCTR1 activity in MDA-MB-231-hCTR1 cells (C) and U87MG-hCTR1 cells (D) was determined by cellular uptake of ^{64}Cu according to incubation time. All data are expressed as mean of triplicate experiments. $^{*}P < 0.05$. $^{**}P < 0.01$. $^{***}P < 0.001$.

complementary DNA preparations were obtained using Superscript III and Oligo(dT) primer (Invitrogen). PCR amplifications of individual complementary DNA were performed (95°C for 5 min; 30 cycles at 95°C for 30 s, 56°C for 30 s; 72°C for 30 s, 72°C for 5 min) using Taq polymerase (iNtRON Biotechnology) and specific primers for *hCTR1* (forward 5′-ATGGATCATTCCCACCATATG-3′ and reverse 5′-TCAATGGCAATGCTCTGTGAT-3′) and *β-actin* (forward 5′-GTGGGGCGCCCCAGGCACCAGGGC-3′ and reverse 5′-CTCCTTAATGTCACGCACGATTTC-3′) genes. The amount of each messenger RNA (mRNA) transcript was normalized to that of *β-actin*.

The procedures for Western blot analysis are described in detail elsewhere (*16*). The protein expression of hCTR1 and β-actin was detected with polyclonal anti-CTR1 antibody (Santa Cruz Biotechnology, Inc.) and monoclonal β-actin antibody (Abcam), respectively.

In Vitro Cytotoxicity Assay

Cell viability was assessed by 3-(4,5-dimethylthiazol-2-yl)-2,5-diphenyltetrazolium bromide (MTT) assay and trypan blue dye exclusion assay. MTT assay was performed according to the manufacturer's recommendations (In Vitro Toxicology Assay Kit, MTT based; Sigma). Briefly, cells were seeded on a 96-well plate in triplicate at a density of 1×10^4 cells/well. After 24 h, cells were treated with different concentrations (0–5 μg/mL) of cisplatin (*Cis*-diaminedichloroplatinum (II) or CDDP; Sigma) for 96 h and the cells were incubated with 10 μL of MTT reagent at room temperature for 3 h. Then, the MTT solution was removed, 100 μL of the detergent reagent was added, and the plate was placed in the dark at room temperature for 20 min. The MTT color development was measured and analyzed by SPECTRA MAX 190 (Molecular Devices) with a single filter (590 nm), and the percentage of viable cells was calculated relative to that of control cells.

Cells were seeded on a 6-well plate in triplicate at a density of 1×10^5 cells/well. After 24 h, cells were treated with different concentrations of CDDP for 72 h. The number of surviving cells was determined by the cell count. Then, 20 μL of trypan blue solution (0.4%, Sigma) was mixed with 20 μL of cell suspension. The suspension was loaded into the C-Chip (Digital Bio.), and cells that stained blue were scored as nonviable.

Biodistribution Study of ^{64}Cu in Tumor-Bearing Mice

The animal experiments were approved by the Institutional Animal Care and Use Committee of the Korea Institute of Radiologic and Medical Sciences. Tumor xenografts were produced in 6-wk-old female BALB/c nude mice by subcutaneous injection of MDA-MB-231 (5×10^6) and MDA-MB-231-hCTR1 (5×10^6) cells suspended in 100 μL of phosphate-buffered saline into the left and right shoulder, respectively. After the tumors were allowed to grow for 2 wk and when the tumors reached a minimum of 7 mm in diameter, the mice were used for biodistribution and imaging studies.

Biodistribution studies were performed in 3 tumor-bearing mice per group. At 2, 4, and 48 h after the intravenous administration of 370 kBq of ^{64}Cu, the mice were sacrificed and their organs removed and weighed, and the radioactivity was measured. Results are expressed as the %ID per gram of tissue (%ID/g).

In Vivo PET Imaging and Autoradiography

At 2, 4, 12, 24, and 48 h after the intravenous injection of 7.4 MBq of ^{64}Cu per animal, mice were placed in a spread prone position and under inhalation anesthesia (isoflurane, 2%) and imaged for 20 min with the microPET-R4 scanner (Concorde Microsystems Inc.) ($n = 3$). Image visualization with decay correction was performed using the ASIPro (Concorde Microsystems Inc.) display software.

Immediately after PET scanning, mice were sacrificed, and tumor tissues were removed and frozen in tissue-freezing medium (FSC22; LEICA Biosystems). After the tissues were decayed for 48 h, sections with a thickness of 20 μm were obtained using a cryostat microtome (CM1800; LEICA Instruments) and exposed on an imaging plate for 24 h. The plates were scanned with BAS-5000 (Fujifilm). Image intensity in the region of interest (ROI) was quantified as units of photostimulated luminescence per square millimeter (PSL/mm^2) using Multi Gauge software (version 3.0; Fujifilm).

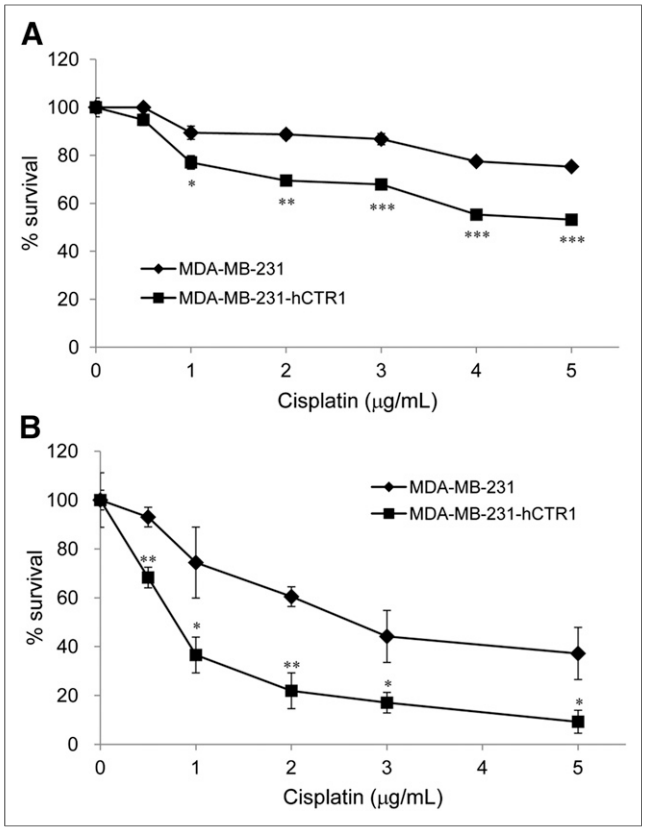

FIGURE 3. Therapeutic efficacy of CDDP treatment induced by hCTR1 expression in MDA-MB-231-hCTR1 cells. Dose-dependent cytotoxicity of CDDP was determined by MTT assay and trypan blue dye exclusion. (A) Dose-dependent cell survival rate (%) of MDA-MB-231 and MDA-MB-231-hCTR1 cells at different doses of CDDP. Cell survival rate was measured by MTT assay at 96 h after CDDP treatment. (B) Cell survival rate was measured by trypan blue dye exclusion assay at 72 h after CDDP treatment. All data are expressed as mean of triplicate experiments. $^{*}P < 0.05$. $^{**}P < 0.01$. $^{***}P < 0.001$.

Immunohistochemistry

Frozen tumor tissues were sectioned at 5 μm, incubated overnight at 4°C with anti-CTR1 antibody (Santa Cruz Biotechnology, Inc., diluted 1:50), and then incubated for 30 min at room temperature with the goat antirabbit IgG-HRP (Santa Cruz Biotechnology, Inc., diluted 1:200). A DAB kit (DAKO) was used for color development. The slides were subsequently counterstained with hematoxylin.

Statistical Analysis

Data were expressed as the mean ± SD. The Student *t* test for unpaired data was used to determine the statistical significance for all comparisons. *P* values of less than 0.05 were considered statistically significant.

RESULTS

Endogenous *hCTR1* RNA Expression in Various Cell Lines

Several human cancer cell lines, including those of hepatoma (HuH-7, HepG2, SK-Hep1), lung cancer (A549, H460), thyroid cancer (SNU-790), colon cancer (HT-29, SW480), ovarian cancer (SK-OV-3), and human breast cancer (BT-474, MCF7), expressed the endogenous *hCTR1* gene as demonstrated by RT-PCR, but the expression levels were different among the cell lines (Fig. 1). HEK293 cells also expressed the *hCTR1* gene. Cancer cells of the same origin such as colon (HT-29, SW480) or breast cancer (BT-474, MCF7) expressed significantly different levels of the *hCTR1* gene.

Generation of Stable Cell Lines Expressing hCTR1 and In Vitro ^{64}Cu Uptake Assay

After selection with blasticidin, we performed a RT-PCR and Western blot analysis to confirm the hCTR1 expression. There were no significant differences between parental cells and transduced cells in cell growth rate (data not shown). In both mRNA and protein level, the enhancement of an hCTR1-specific band was detected in MDA-MB-231-hCTR1 or U87MG-hCTR1 cells, compared with parental cells (Figs. 2A and 2B). This result suggested that *hCTR1* gene expression increases by lentiviral gene transfer in MDA-MB-231-hCTR1 or U87MG-hCTR1 cells. ^{64}Cu uptake induced by hCTR1 expression was also increased in transduced cells, compared with parental cells (Figs. 2C and 2D). Although cellular ^{64}Cu uptake in vitro and tumor ^{64}Cu uptake measured by $^{64}CuCl_2$ PET in vivo represented a total ^{64}Cu uptake mediated by both endogenous and exogenous hCTR1 expressed in MDA-MB-231-hCTR1 or U87MG-hCTR1 cells, the time-dependent increase of ^{64}Cu uptake in these 2 cell lines relative to ^{64}Cu uptake in their parental cells provided strong evidence for exogenous hCTR1-mediated increase of ^{64}Cu uptake in the MDA-MB-231-hCTR1 and U87MG-hCTR1 cells (Figs. 2C and 2D).

Therapeutic Efficacy of Cisplatin Treatment in MDA-MB-231-hCTR1 Cells

The survival rates of MDA-MB-231-hCTR1 and MDA-MB-231 cells were determined by MTT assay after CDDP treatment for 96 h (Fig. 3A) and trypan blue dye exclusion assay after CDDP treatment for 72 h (Fig. 3B). A dose-dependent toxicity was observed after continuous exposure to CDDP. The viability of MDA-MB-231-hCTR1 cells decreased more rapidly than that of MDA-MB-231 cells after CDDP exposure. In the trypan blue dye exclusion assay, the 50% lethal dose of CDDP was 0.74 μg/mL for MDA-MB-231-hCTR1 cells, whereas the 50% lethal dose of CDDP was 2.67 μg/mL (3-fold higher) for MDA-MB-231 cells. MDA-MB-231-hCTR1 cells were more sensitive to CDDP treatment than MDA-MB-231 cells.

Small-Animal PET Imaging, Autoradiography, and Immunohistochemistry of Excised Tumors

The xenograft models bearing MDA-MB-231 and MDA-MB-231-hCTR1 tumors in the left and right shoulder, respectively, were imaged using a small-animal PET scanner after a tail vein injection of 7.4 MBq of ^{64}Cu (Fig. 4A). As shown in Figure 4, the PET images clearly demonstrate a higher ^{64}Cu uptake in the MDA-MB-231-hCTR1 tumor than in the MDA-MB-231 tumor. The ^{64}Cu uptake in the MDA-MB-231 tumor was 1.368 ± 0.316 %ID/g and that in the MDA-MB-231-hCTR1 tumor was 3.574 ± 0.571 %ID/g at 48 h after injection of ^{64}Cu. The ^{64}Cu uptake in the MDA-MB-231-hCTR1 tumor exhibited an increasing pattern with progression of time, but that in the MDA-MB-231 tumor showed a steady-state pattern (Fig. 4B). The highest uptake of ^{64}Cu was observed in the liver, which is the major organ for copper metabolism. But the ^{64}Cu uptake was steeply decreased with progression of time. Therefore, small-animal PET imaging revealed a greater accumulation of ^{64}Cu in the MDA-MB-231-hCTR1 tumor than in the MDA-MB-231 tumor because of the

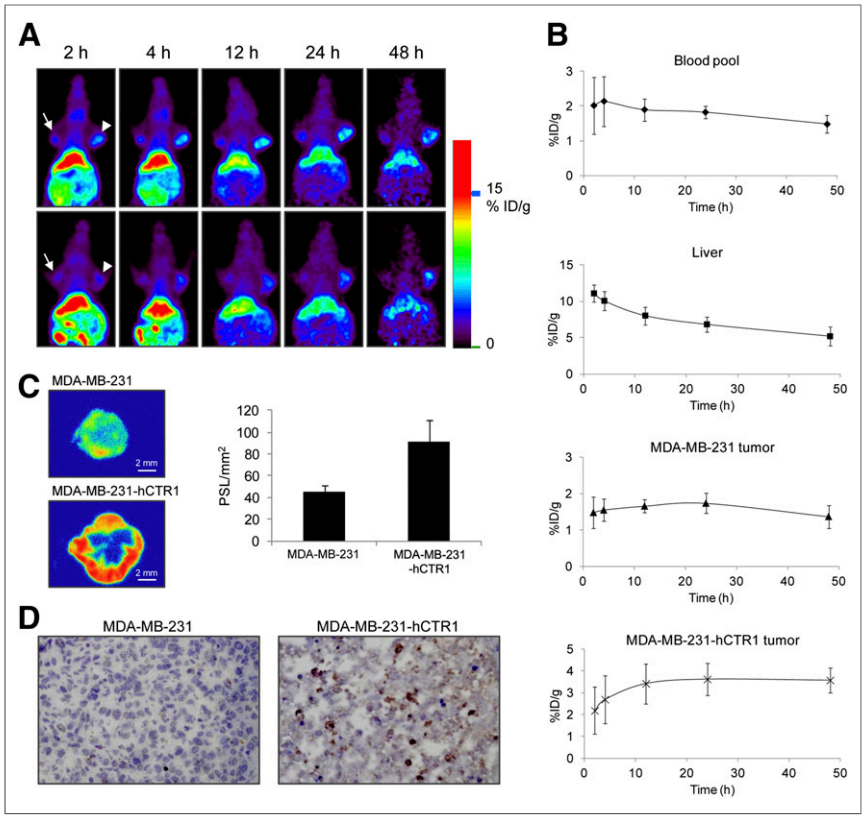

FIGURE 4. Small-animal PET images and autoradiographs of MDA-MB-231 and MDA-MB-231-hCTR1 tumors after injection of ^{64}Cu. (A) Representative PET images of xenografted mice bearing MDA-MB-231 (arrow) and MDA-MB-231-hCTR1 (arrowhead) tumors after tail vein injection of ^{64}Cu (n = 3). PET images were obtained at 2, 4, 12, 24, and 48 h after ^{64}Cu injection. (B) Time–activity curves of blood pool, liver, MDA-MB-231 tumor, and MDA-MB-231-hCTR1 tumor were calculated on PET images. Blood-pool activity was obtained from ROI of heart region. Time course of radioactivity was obtained by ROI analysis and presented as %ID/g. (C) Autoradiopraphs of MDA-MB-231 and MDA-MB-231-hCTR1 tumors. After acquisition of PET images, mice were euthanized. Tumor sections were exposed to image plate for scanning and quantification of ROI. (D) Anti-CTR1 immunohistochemistry of slices from MDA-MB-231 (left) and MDA-MB-231-hCTR1 (right) tumor tissues (original magnification, ×400).

expression of *hCTR1* gene. Autoradiography showed a higher ^{64}Cu uptake in the MDA-MB-231-hCTR1 tumor than in the MDA-MB-231 tumor (Fig. 4C). The ROI in the digitized section photographs was 44.705 ± 5.904 and 90.85 ± 19.658 PSL/mm^2 in the MDA-MB-231 and MDA-MB-231-hCTR1 tumors, respectively. The relative activity ratio of the MDA-MB-231-hCTR1 tumor to the MDA-MB-231 tumor was 2.03. Therefore, higher ^{64}Cu accumulation was observed in the MDA-MB-231-hCTR1 tumor. Immunohistochemistry revealed that there was no or little hCTR1 immune reactivity signal in the MDA-MB-231 tumor tissue, but there was a heterogeneous pattern of hCTR1 expression in the MDA-MB-231-hCTR1 tumor tissue showing intense spots on some of cells (Fig. 4D).

Biodistribution

The biodistribution of ^{64}Cu was presented as the %ID/g in various organs including xenografted tumors (Fig. 5). The ^{64}Cu uptake in the MDA-MB-231 tumor and the MDA-MB-231-hCTR1 tumor was 2.581 ± 0.254 and 5.373 ± 1.098 %ID/g, respectively, at 48 h after ^{64}Cu injection ($P < 0.05$). The relative radioactivity ratio of the MDA-MB-231-hCTR1 tumor to the MDA-MB-231 tumor was 2.08. Therefore, a higher accumulation and longer retention of ^{64}Cu was observed in the MDA-MB-231-hCTR1 tumor. These results were also consistent with small-animal PET imaging (Fig. 4).

DISCUSSION

CTR1 has been identified to play a major role in copper transport in mammalian cells and has been shown to be essential for murine embryonic development in knock-out studies of mCTR1 alleles (*6,17*). Lee et al. characterized the copper transport activity of hCTR1 by expressing hCTR1 in an embryonic kidney cell line (HEK293) using ^{64}Cu from the Mallinckrodt Institute of Radiology, Washington University. They confirmed that CTR1 plays a role in copper uptake across the plasma membrane (*7*).

Zhou et al. reported that *hCTR1* mRNA was detectable by Northern blot analysis in 16 major human organs (*5*). Holzer et al. determined the pattern of hCTR1 expression in normal and malignant human tissues by standard immunohistochemical techniques (*18*). They suggested that hCTR1 expressions in malignant tissues reflect the levels found in their normal tissue counterparts—such as α cells of the pancreatic islets, enteroendocrine cells of the gastric mucosa and bronchioles, C cells of the thyroid, and a subset of cells in the anterior pituitary gland—and that hCTR1 expression was not commonly enhanced by transformation. Lee et al. found a lower expression of *CTR1* mRNA in 40 ovarian cancer cell samples against normal ovarian tissue by real-time PCR with statistically significant differences (*19*). Therefore, the hCTR1 expression may not be commonly enhanced or repressed by the cancer transformation process and influenced by a tissue counterpart of a cancer. In our study, human cancer cell lines derived from various tissues expressing the *hCTR1* gene were assessed by RT-PCR (Fig. 1).

Peng et al. reported that human prostate cancer xenografts in mice were detected by PET using ^{64}Cu as a probe and that the ^{64}Cu uptake in the tumor xenograft was approximately 5 %ID/g at 24 h after injection according to the biodistribution study (*20*). A similar experiment was presented by Zhang et al. to propose the possibility of assessment of hepatocellular carcinoma by PET imaging. The ^{64}Cu uptake in a hepatocellular carcinoma xenograft was 2.7 ± 0.6 %ID/g as measured by PET quantitative analysis (*21*). Recently, Qin et al. reported that CTR1-expressing malignant melanoma can be visualized by PET and treated by $^{64}CuCl_2$ as a theranostic radionuclide (*22*). In the present study, we obtained PET images for ^{64}Cu uptake via exogenous gene expression as well as endogenous gene expression of hCTR1 and compared the ^{64}Cu uptake kinetics in xenografted tumors as determined by PET quantitation analysis and biodistribution in various organs including

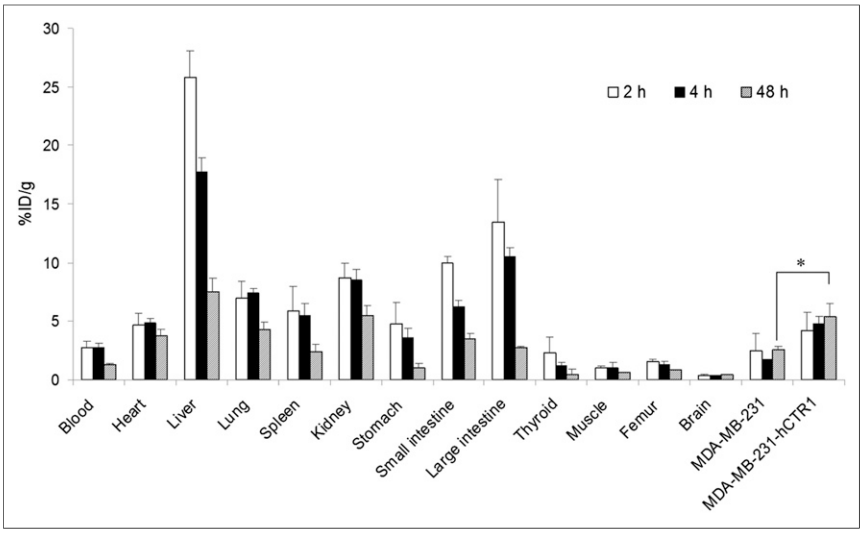

FIGURE 5. Biodistribution study after injection of ^{64}Cu. At 2, 4, and 48 h after injection of ^{64}Cu into tumor xenograft mice, mice were euthanized and radioactivity in organs was measured ($n = 3$). Radioactivity in tissues is expressed as %ID/g. $^{*}P < 0.05$.

tumors (Figs. 4B and 5). The uptake kinetics in the exogenous gene-expressing tumor (MDA-MB-231-hCTR1) were clearly different from those in the MDA-MB-231 tumor, in which the ^{64}Cu uptake in the MDA-MB-231 tumor as well as in the other organs declined with progression of time.

However, there are some considerations to apply *hCTR1* gene as a PET reporter gene. First, recently it was reported that tumor growth could be inhibited by knockdown of hCTR1 expression (*23,24*). Second, further research is needed about some effects on expression of other copper efflux transporter or molecular chaperons and mechanisms to maintain the cellular copper homeostasis by hCTR1 overexpression. Third, because of potential copper toxicity induced by hCTR1 overexpression, use of hCTR1 as a reporter gene for tracking gene delivery to nonmalignant cells should be applied restrictively.

In mammalian cells, copper exporter (ATP7A, ATP7B) and CTR1 could serve as a target for therapeutic effects of platinum-containing drugs (*25,26*). Because hCTR1 can transport platinum-containing drugs such as CDDP and CDDP-like drugs, hCTR1 overexpression was associated with favorable therapeutic effects of a CDDP-based cancer chemotherapy (*27*). As shown in Figure 3, our results are in accordance with aforementioned reports. However, Holzer et al. reported that an enhanced expression of hCTR1 in ovarian cancer cells induced higher accumulation of CDDP and copper but only a marginal increase in the cytotoxicity of CDDP due to improper intracellular localization of CDDP (*14*). Therefore, the cytotoxicity induced by CTR1 expression and CDDP in cancer cells might still be controversial (*28–30*), and this issue should be resolved by performing a further study.

CONCLUSION

We successfully produced a lentiviral vector expressing *hCTR1* gene and demonstrated increased ^{64}Cu uptake mediated by overexpression of hCTR1 in breast cancer cells in vitro and in vivo. The findings of this proof-of-concept study support further study of the potential use of *hCTR1* as a new reporter gene for tracking gene delivery in vivo with PET using $^{64}CuCl_2$.

DISCLOSURE

The costs of publication of this article were defrayed in part by the payment of page charges. Therefore, and solely to indicate this fact, this article is hereby marked "advertisement" in accordance with 18 USC section 1734. This work was supported by the Korea Science and Engineering Foundation (KOSEF) grant funded by the Korea government (MEST) (NRF-2012M2A2A7013480). None of the authors have any financial and personal relationships with other people or organizations that inappropriately influence our work. No other potential conflict of interest relevant to this article was reported.

REFERENCES

1. Wessling-Resnick M. Understanding copper uptake at the molecular level. *Nutr Rev.* 2002;60:177–179.
2. Kaler SG, Holmes CS, Goldstein DS, et al. Neonatal diagnosis and treatment of Menkes disease. *N Engl J Med.* 2008;358:605–614.
3. Das SK, Ray K. Wilson's disease: an update. *Nat Clin Pract Neurol.* 2006;2:482–493.
4. Dancis A, Yuan DS, Haile D, et al. Molecular characterization of a copper transport protein in S. cerevisiae: an unexpected role for copper in iron transport. *Cell.* 1994;76:393–402.
5. Zhou B, Gitschier J. hCTR1: a human gene for copper uptake identified by complementation in yeast. *Proc Natl Acad Sci USA.* 1997;94:7481–7486.
6. Lee J, Prohaska JR, Dagenais SL, Glover TW, Thiele DJ. Isolation of a murine copper transporter gene, tissue specific expression and functional complementation of a yeast copper transport mutant. *Gene.* 2000;254:87–96.
7. Lee J, Pena MM, Nose Y, Thiele DJ. Biochemical characterization of the human copper transporter Ctr1. *J Biol Chem.* 2002;277:4380–4387.
8. Kang JH, Chung JK. Molecular-genetic imaging based on reporter gene expression. *J Nucl Med.* 2008;49(suppl 2):164S–179S.
9. Shokeen M, Wadas TJ. The development of copper radiopharmaceuticals for imaging and therapy. *Med Chem.* 2011;7:413–429.
10. Kang JH, Chung JK, Lee YJ, et al. Establishment of a human hepatocellular carcinoma cell line highly expressing sodium iodide symporter for radionuclide gene therapy. *J Nucl Med.* 2004;45:1571–1576.
11. Knoop K, Schwenk N, Dolp P, et al. Stromal targeting of sodium iodide symporter using mesenchymal stem cells allows enhanced imaging and therapy of hepatocellular carcinoma. *Hum Gene Ther.* 2013;24:306–316.
12. Haddad D, Zanzonico PB, Carlin S, et al. A vaccinia virus encoding the human sodium iodide symporter facilitates long-term image monitoring of virotherapy and targeted radiotherapy of pancreatic cancer. *J Nucl Med.* 2012;53:1933–1942.
13. Larson CA, Blair BG, Safaei R, Howell SB. The role of the mammalian copper transporter 1 in the cellular accumulation of platinum-based drugs. *Mol Pharmacol.* 2009;75:324–330.
14. Holzer AK, Samimi G, Katano K, et al. The copper influx transporter human copper transport protein 1 regulates the uptake of cisplatin in human ovarian carcinoma cells. *Mol Pharmacol.* 2004;66:817–823.
15. Kim JY, Park H, Lee JC, et al. A simple Cu-64 production and its application of Cu-64 ATSM. *Appl Radiat Isot.* 2009;67:1190–1194.
16. Kim KI, Kang JH, Chung JK, et al. Doxorubicin enhances the expression of transgene under control of the CMV promoter in anaplastic thyroid carcinoma cells. *J Nucl Med.* 2007;48:1553–1561.

17. Kuo YM, Zhou B, Cosco D, Gitschier J. The copper transporter CTR1 provides an essential function in mammalian embryonic development. *Proc Natl Acad Sci USA.* 2001;98:6836–6841.
18. Holzer AK, Varki NM, Le QT, Gibson MA, Naredi P, Howell SB. Expression of the human copper influx transporter 1 in normal and malignant human tissues. *J Histochem Cytochem.* 2006;54:1041–1049.
19. Lee YY, Choi CH, Do IG, et al. Prognostic value of the copper transporters, CTR1 and CTR2, in patients with ovarian carcinoma receiving platinum-based chemotherapy. *Gynecol Oncol.* 2011;122:361–365.
20. Peng F, Lu X, Janisse J, Muzik O, Shields AF. PET of human prostate cancer xenografts in mice with increased uptake of $^{64}CuCl_2$. *J Nucl Med.* 2006;47:1649–1652.
21. Zhang H, Cai H, Lu X, Muzik O, Peng F. Positron emission tomography of human hepatocellular carcinoma xenografts in mice using copper (II)-64 chloride as a tracer with copper (II)-64 chloride. *Acad Radiol.* 2011;18:1561–1568.
22. Qin C, Liu H, Chen K, et al. Theranostics of malignant melanoma with $^{64}CuCl_2$. *J Nucl Med.* 2014;55:812–817.
23. Cai H, Wu JS, Muzik O, Hsieh JT, Lee RJ, Peng F. Reduced ^{64}Cu uptake and tumor growth inhibition by knockdown of human copper transporter 1 in xenograft mouse model of prostate cancer. *J Nucl Med.* 2014;55:622–628.
24. Brady DC, Crowe MS, Turski ML, et al. Copper is required for oncogenic BRAF signalling and tumorigenesis. *Nature.* 2014;509:492–496.
25. Gupta A, Lutsenko S. Human copper transporters: mechanism, role in human diseases and therapeutic potential. *Future Med Chem.* 2009;1:1125–1142.
26. Howell SB, Safaei R, Larson CA, Sailor MJ. Copper transporters and the cellular pharmacology of the platinum-containing cancer drugs. *Mol Pharmacol.* 2010;77:887–894.
27. More SS, Akil O, Ianculescu AG, Geier EG, Lustig LR, Giacomini KM. Role of the copper transporter, CTR1, in platinum-induced ototoxicity. *J Neurosci.* 2010;30:9500–9509.
28. Beretta GL, Gatti L, Tinelli S, et al. Cellular pharmacology of cisplatin in relation to the expression of human copper transporter CTR1 in different pairs of cisplatin-sensitive and -resistant cells. *Biochem Pharmacol.* 2004;68:283–291.
29. Martens-de Kemp SR, Dalm SU, Wijnolts FM, et al. DNA-bound platinum is the major determinant of cisplatin sensitivity in head and neck squamous carcinoma cells. *PLoS ONE.* 2013;8:e61555.
30. Ivy KD, Kaplan JH. A re-evaluation of the role of hCTR1, the human high-affinity copper transporter, in platinum-drug entry into human cells. *Mol Pharmacol.* 2013;83:1237–1246.